



Nanomechanical properties of GaSe thin films deposited on Si(111) substrates by pulsed laser deposition

Sheng-Rui Jian^{a,*}, Jenh-Yih Juang^b, Chih-Wei Luo^b, Shin-An Ku^b, Kaung-Hsiung Wu^b

^a Department of Materials Science and Engineering, I-Shou University, Kaohsiung 840, Taiwan

^b Department of Electrophysics, National Chiao Tung University, Hsinchu 300, Taiwan

ARTICLE INFO

Article history:

Received 10 June 2012

Received in revised form 17 July 2012

Accepted 19 July 2012

Available online 27 July 2012

Keywords:

GaSe thin films

XRD

Nanoindentation

Hardness

ABSTRACT

The correlations between the crystalline structure and mechanical properties of GaSe thin films were investigated by means of X-ray diffraction (XRD) and nanoindentation techniques. The GaSe thin films were deposited on Si(111) substrates deposited at various deposition temperatures using pulsed laser deposition (PLD). The XRD results indicate that all the GaSe thin films are pure hexagonal phase with highly (0001)-oriented characteristics. Nanoindentation results revealed apparent discontinuities (so-called multiple “pop-in” events) in the load-displacement curve, while no discontinuity was observed in the unloading segment of the load-displacement curve. The hardness and Young's modulus of GaSe thin films determined by the continuous stiffness measurements (CSM) method indicated that both mechanical parameters increased with the increasing deposition temperature with the hardness and the Young's modulus being increased from 1.2 ± 0.1 to 1.8 ± 0.1 GPa and from 39.6 ± 1.2 to 68.9 ± 2.7 GPa, respectively, as the deposition temperature was raised from 400 to 475 °C. These results suggest that the increased grain size might have played a prominent role in determining the mechanical properties of the PLD-derived GaSe thin films.

© 2012 Elsevier B.V. All rights reserved.

1. Introduction

Recently, enormous research interest has been focused on layered III–VI semiconducting compounds. The burst of interest has partly arisen from the emergent physical properties associated with the quasi-two-dimensional natures of these compounds and partly because of their attractive technological applications. Among the family of layered III–VI semiconductors, gallium selenide (GaSe) is one of the materials subjected to extensive researches, owing to the peculiar nonlinear optical properties exhibited in this material. A quadruple layer of GaSe consists of two Ga and two Se sub-layers in the sequence of Se–Ga–Ga–Se, where the Se–Ga and Ga–Ga bonds are covalent within the layers and the Se–Se bond between adjacent quadruple layers is due to van der Waals forces [1,2]. GaSe thin films have been successfully prepared by using vapour deposition [3,4] and molecular beam epitaxy [5,6] techniques. Compared to these growth techniques, pulsed laser deposition (PLD) is a relatively new technique used widely for the growth of multi-element materials such as ferroelectrics [7] and superconductors [8] due to its high-energy flux and capability of preserving the stoichiometries from the target materials. The growth rate achieved by PLD can be easily varied

by adjusting the repetition rate and energy density of laser pulses, which is useful for both atomic level investigations and for growing thick layer of films within reasonable time durations. Moreover, the PLD method can also offer the potential of growing high-quality thin films at relatively lower substrate temperatures as compared to other techniques. Therefore, we have tried to grow the GaSe thin films by using PLD method in this study.

Over the last several years, there have been growing interest of fabricating GaSe-based optical and electronic devices using the established thin-film technologies widely adopted in semiconductor industries [9,10]. However, while most of the researches have been concentrated on the devices' electrical and optical characteristics, the investigations on the mechanical properties of GaSe thin films have not drawn equal attention, albeit that an accurate assessment on the mechanical properties of GaSe thin films is also very crucial in order to obtain the optimal robustness and functionalities of the targeted devices. To this regard, nanoindentation has been widely used for characterizing the mechanical properties of various nanomaterials [11–13] and thin films [14–16], due to its high sensitivity and excellent resolution for obtaining the hardness, Young's modulus and elastic/plastic deformation behaviors in a relatively easier fashion. The primary focus of the present study is to provide insights into the structural and nanomechanical properties of GaSe thin films deposited on Si(111) substrates at various deposition temperatures by PLD

* Corresponding author. Tel.: +886 7 6577711x3130; fax: +886 7 6578444.

E-mail address: srjian@gmail.com (S.-R. Jian).

with the aids of X-ray diffraction (XRD) and nanoindentation techniques.

2. Experimental details

The GaSe thin films investigated in this study were deposited on Si(111) substrates at the deposition temperatures of 400, 425 and 475 °C, respectively, by pulsed laser deposition (PLD). The target used was a GaSe single crystal grown by the vertical Bridgeman method. All of the GaSe thin films are about 200 nm thick. The structural features of GaSe thin films were examined by X-ray diffraction (XRD; Bruker D8 Advance TXS with Cu-K α radiation, $\lambda = 1.5406 \text{ \AA}$).

The nanoindentation measurements were performed on a Nanoindenter MTS NanoXP[®] system (MTS Cooperation, Nano Instruments Innovation Center, TN, USA) with a pyramid-shaped Berkovich-type diamond indenter tip, whose radius of curvature is 50 nm. The mechanical properties (the hardness and Young's modulus) of GaSe thin films were measured by nanoindentation with a continuous stiffness measurements (CSM) technique [17]. In this technique, a small sinusoidal load with known frequency and amplitude was superimposed onto the quasi-static load. It results in a modulation of the indenter displacement that is phase shifted in response to the excitation force. The stiffness, S of the material, and the damping, wC , along indentation loading can be respectively calculated using Eqs. (1) and (2) expressed below.

$$S = \left[\frac{1}{\frac{P_{\max}}{h(w)} \cos \Phi - (K_s - mw^2) - K_f^{-1}} \right]^{-1} \quad (1)$$

$$wC = \frac{P_0}{h(w)} \sin \Phi \quad (2)$$

where P_{\max} and $h(w)$ are denoted as the driving force and the displacement response of the indenter, respectively; Φ is the phase angle between P_{\max} and $h(w)$; m is the mass of the indenter column; K_s is spring constant at the vertical direction; K_f is frame stiffness; m , K_s and K_f are all constant values for specified indentation system; w is angular speed which equals to $2\pi f$; f is the driven frequency of the ac signal of 45 Hz for this work, which is used to avoid the sensitivity to thermal drift. The loading resolution of the system was 50 nN. The hardness and elastic modulus are, then, calculated by putting the obtained stiffness data into Eqs. (3) and (4) shown below, respectively.

$$H = \frac{P_{\max}}{A_c} \quad (3)$$

$$\frac{E}{1 - \nu^2} = \frac{\sqrt{\pi}}{2} \frac{1}{\sqrt{A_c}} S \quad (4)$$

Here, ν is the Poisson's ratio of the material and is set to be 0.25 for the current analysis, and A_c is contact area when the material in contact with indenter being loaded at P_{\max} . In this way, the hardness and modulus as a function of penetration depth can be determined for a single loading/unloading cycle [18].

The area function, which is used to calculate contact area, A_c , from contact depth, h_c , was carefully calibrated by using fused silica as the standard sample prior to the nanoindentation experiments. The nanoindentation tests were carried out in the following sequence: first of all, the Berkovich indenter was brought into contact with the surface at a constant strain rate of 0.05 s^{-1} until $\sim 80 \text{ nm}$ of penetration was achieved. The load was then held at the maximum value for 10 s in order to determine the creep behavior. The Berkovich indenter was then withdrawn from the surface at the same rate until 10% of the maximum load was reached. This constant strain rate was chosen such that the strain-hardening effect can be avoided during the measurements. At least 20 indents were performed on each GaSe thin film. The nanoindentations were sufficiently spaced to prevent each test from mutual interactions.

3. Results and discussion

The XRD results of the PLD-derived GaSe thin films with various deposition temperatures are shown in Fig. 1. It can be found that the intensity of (004) diffraction peak increases and the full width at half maximum (FWHM) of the (004) peak becomes narrower with the increasing deposition temperature and there is no other impurity phases or trace of amorphous regions discernible even from the diffraction pattern for film deposited at the lowest temperature of 400 °C. Moreover, the obtained corresponding d -spacing values are in good agreement with that reported for hexagonal-structured GaSe (JCPDS 37-0931). These indicate that all of the PLD-derived GaSe thin films are highly (001)-oriented

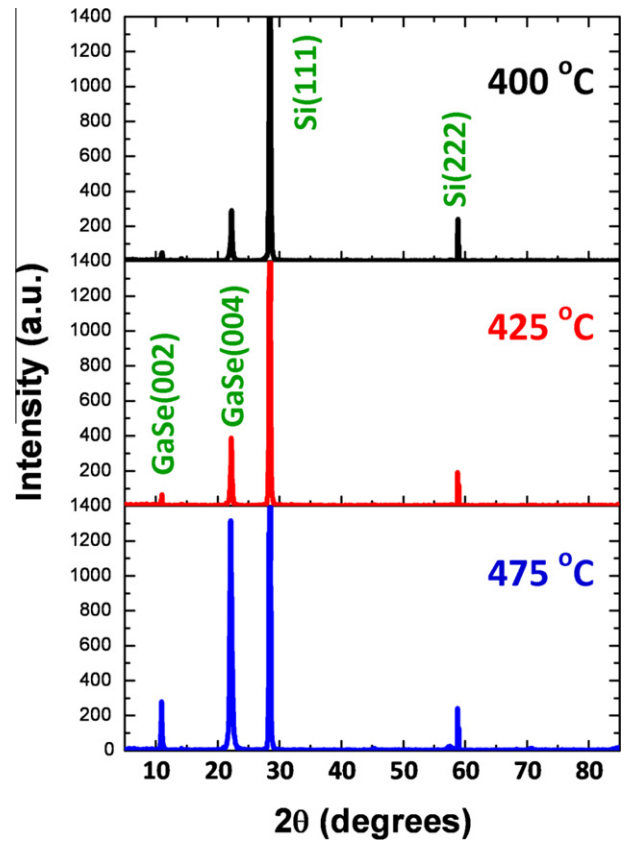


Fig. 1. XRD patterns of GaSe thin films at various deposited temperatures.

and the crystalline quality is progressively improved as the deposition temperature is increased.

The grain size, D , of the corresponding thin films can be estimated according to the Scherrer's equation [19]:

$$D = \frac{0.9\lambda}{B \cos \theta} \quad (5)$$

where λ , B and θ are the X-ray wavelength, the FWHM of GaSe (004)-oriented peak and the Bragg diffraction angle, respectively. The estimated grain sizes for GaSe thin films deposited at 400, 425 and 475 °C are 23.5, 30.8 and 51.2 nm, respectively.

The typical load-displacement curve for GaSe thin films deposited at the deposition temperature of 475 °C is displayed in Fig. 2(a). The load-displacement response obtained by nanoindentation contains information about the elastic and plastic deformation of the indented materials. Therefore, it is often regarded as a "fingerprint" of the film properties under identification. Mechanical properties, such as the hardness and Young's modulus, can be readily extracted from the load-displacement curves like those displayed in Fig. 2(b) and (c).

The hardness and Young's modulus as a function of penetration depth obtained by using the analyses described above are illustrated in Fig. 2(b) and (c), respectively, for GaSe thin films deposited at various temperatures. As shown in Fig. 2(b), although the hardness-displacement plots exhibiting substantial differences in details, the behaviors can be roughly divided into two stages. Namely, the hardness initially increases with the penetration depth to a maximum value and then subsequently decreases to a constant value. The increase in hardness at small penetration depth is usually attributed to the transition between purely elastic to elastic/plastic contact and at this stage the measured mean contact pressure does not accurately represent the real hardness of the

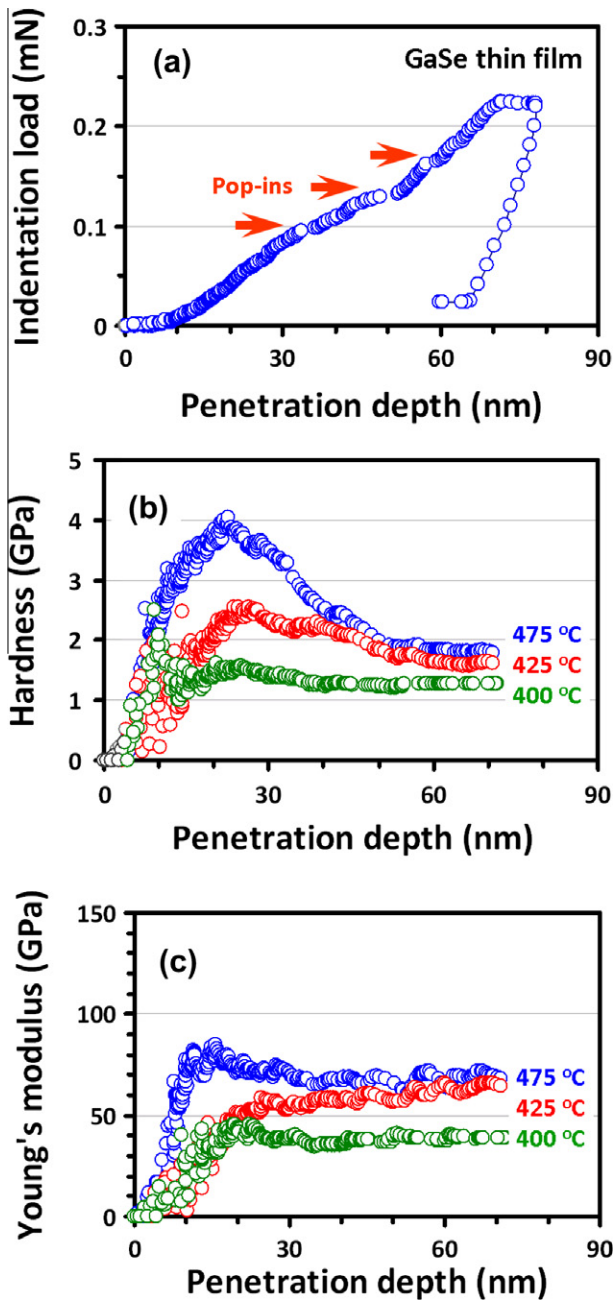


Fig. 2. Nanoindentation measurement results: (a) a typical load-displacement curve for GaSe thin film at 475 °C; (b) hardness–Displacement and (c) Young's modulus–Displacement curves for GaSe thin films deposited at different temperatures.

material. Only under the condition of a fully developed plastic zone does the mean contact pressure represent the hardness. When there is no plastic zone, or only partially formed plastic zone, the

mean contact pressure is less than the nominal hardness [18]. After the first stage, the hardness decreases and reaches a constant value, which could be regarded as intrinsic properties of the films. The obtained hardness for the GaSe thin films at the deposition temperatures of 400, 425 and 475 °C are 1.2 ± 0.1 , 1.5 ± 0.2 and 1.8 ± 0.1 GPa, respectively. Furthermore, as displayed in Fig. 2(c), the Young's modulus as a function of the penetration depth determined using the method of Oliver and Pharr [18] also shows a similar tendency as that of film hardness. The values of Young's modulus for GaSe thin films are 39.6 ± 1.2 , 61.7 ± 3.8 and 68.9 ± 2.7 GPa at the deposition temperatures of 400, 425 and 475 °C, respectively. Comparing to the hardness of 2.0 ± 0.4 GPa obtained from the bulk single crystal of GaSe [20], the hardness values of the present films appear to be considerably smaller. Nevertheless, the values of Young's modulus of the films are substantially larger than the bulk value of 33 ± 3 GPa. The reason for these seemingly anomalous behaviors in mechanical properties is not clear at present and further microstructural analyses are certainly needed. However, the grain size and associated effects from grain boundaries presumably might have been playing some roles. It has been pointed out that, due to the influences of surface stress effect [21,22], the mechanical properties of materials can be very much size-dependent in the nanoscale regime. In particular, in a polycrystalline material where the dislocation activities are drastically suppressed due to the reduced grain size, the deformation behavior will be dominated by grain boundary sliding and/or grain rotations, which in turn would give rise to the manifestations of inverse Hall–Petch effect [23]. Namely, the material becomes stronger when the grain size is larger. In fact, similar behaviors have been experimentally observed in Ga-doped ZnO films reported elsewhere [14].

Turning back to Fig. 2(a), it is evident that there exist multiple discontinuities along the loading course (indicated by the arrows). These features are apparently reflecting certain types of the plastic deformation processes in the material and are generally referred as multiple “pop-ins”. The “pop-ins” are ubiquitously observed in materials with hexagonal crystalline structures and usually attributed to indentation-induced nucleation of dislocations [24–26]. On the other hand, the reversal discontinuity occurs during unloading, the so-called “pop-out” event, commonly observed in Si is conceived to intimately relate to pressure-induced phase transformation [27,28], which is not observed here. Within the context of the abovementioned scenarios, it is suggestive that the first pop-in event may reflect the transition from perfectly elastic to plastic deformation. In other words, it is the onset of plasticity in GaSe thin film. It is well known that the theoretical stress for the occurrence of plastic deformation can be approximated as $\tau_c \approx G/10$ [29], which corresponds to the critical stress for initiating the generation of dislocations. Here, ($G = E/2(1 + \nu)$) is the shear modulus of GaSe thin films. According to the Tresca criterion and the Hertzian contact model for the indentation of a semi-infinite elastic material the maximum shear stress, τ_{\max} , can be calculated as [30]:

$$\tau_{\max} = 0.31 \left(\frac{6P_c E^2}{\pi^3 R^2} \right)^{1/3} \quad (6)$$

Table 1
Mechanical properties of GaSe thin films deposited at various temperatures.

GaSe thin films [#] Deposition temperature	D (nm)	H (GPa)	E_{film} (GPa)	τ_{\max} (GPa)
400 °C	23.5	1.2 ± 0.1	39.6 ± 1.2	0.4 ± 0.1
425 °C	30.8	1.5 ± 0.2	61.7 ± 3.8	0.5 ± 0.1
475 °C	51.2	1.8 ± 0.1	68.9 ± 2.7	0.6 ± 0.1
		2.0 ± 0.4 [23]	33 ± 3 [23]	

[#] This study.

where P_c is the critical load at which the pop-in occurs during nanoindentation process and R is the radius of the tip of the indenter. The maximum shear stresses thus obtained together with the parameters characterizing the microstructural and mechanical properties of GaSe thin film are summarized in Table 1.

Finally, the total number of activated dislocations, N , for a pop-in event can also be estimated from the dislocation density, ρ , using the following expressions [31]:

$$N \approx 0.09\rho R^2, \quad \text{where } \rho \approx \delta_{pop-in} \cdot \frac{21.62}{\pi R^2 h} \cdot \left(\frac{4}{3\pi} \cdot \frac{E}{G}\right)^2 \quad (7)$$

where h is the indentation depth and δ_{pop-in} is the width of pop-in event. From Fig. 2(a), $\delta_{pop-in} \approx 1.2$ nm, $h \approx 80$ nm are obtained and by inserting these numbers together with $G \approx 28$ GPa into Eq. (7), a dislocation density of $\sim 4.2 \times 10^9$ cm⁻² is obtained. This also implies that the total number of activated dislocations within the area directly underneath the indenter is only about 0.0095. Lorenz et al. [29] proposed that when the number of the activated dislocations is smaller than 0.01, there is a very high probability to observe the pop-in event experimentally, which is in good agreement with the observation and calculations based on the results shown in Fig. 2(a). It is, thus, quite plausible to state that the observed pop-in events presented here are predominantly due to the pressure-induced homogeneous nucleation of dislocations. However, the observed inverse Hall–Petch effect behavior described in previous paragraphs suggests that an alternative interpretation based on the grain boundary sliding and/or grain rotation might be also possible. In fact, the low N value of ~ 0.0095 obtained above further suggests the latter mechanism might have played the more important role in determining the observed deformation behavior than did the homogeneous dislocation nucleation scenario.

4. Conclusions

We have used the XRD and nanoindentation techniques investigate the structural features and nanomechanical properties of GaSe thin films deposited on Si(1 1 1) substrates at three different temperatures by PLD. The main findings are summarized as following:

1. XRD indicated that the crystal structure of the obtained GaSe thin films is purely hexagonal phase and the films are essentially (001)-oriented. In addition, the grain size of the GaSe thin films deposited at 400, 425 and 475 °C are 23.5, 30.8 and 51.2 nm, respectively.
2. Nanoindentation results indicate that the film hardness increases with the increasing deposition temperature: from 1.2 ± 0.1 GPa for films deposited at 400 °C to 1.8 ± 0.1 GPa for those deposited at 475 °C. The Young's modulus of the GaSe films also showed similar trend, namely $E = 68.9 \pm 2.7$ GPa for films deposited at 475 °C, while $E = 39.6 \pm 1.2$ GPa for that deposited at 400 °C. It is noted that, while the obtained film hardness is smaller than the bulk value of 2.0 ± 0.4 GPa, the Young's modulus of the films are all substantially larger than the bulk value of 33 ± 3 GPa.

3. Clear evidences of dislocation nucleation-induced multiple pop-ins in the load–displacement curve during nanoindentation measurements are observed, and the estimations made based on the experimental results show good agreement with the theoretical predictions.

Acknowledgements

This work was partially supported by the National Science Council of Taiwan, under Grant Nos. NSC101-2221-E-214-017 and NSC100-2221-E-214-024. JJY is partially supported by the NSC of Taiwan and the MOE-ATU program operated at NCTU. Author likes to thank Dr. Y.-S. Lai and Dr. P.-F. Yang (Central Product Solutions, Advanced Semiconductor Engineering, Taiwan) for their technical supports.

References

- [1] J. Pellicer-Porres, A. Segura, Ch. Ferrer, V. Munoz, A. San Miguel, A. Polian, J.P. Itie, M. Gauthier, S. Pascarelli, Phys. Rev. B 65 (2002) 174103.
- [2] S.K. Tripathi, S. Gupta, F.I. Mustafa, N. Goyal, G.S.S. Saini, J. Phys. D: Appl. Phys. 42 (2009) 185404.
- [3] E.G. Gillan, A.R. Barron, Chem. Mater. 9 (1997) 3037.
- [4] S. Gupta, F.I. Mustafa, N. Goyal, S.K. Tripathi, Appl. Phys. A 103 (2011) 477.
- [5] R. Rudolph, C. Pettenkofer, A. Klein, W. Jaegermann, Appl. Surf. Sci. 167 (2000) 122.
- [6] H.F. Jurca, I. Mazzaro, W.H. Schreiner, D.H. Mosca, M. Eddrief, V.H. Etgens, Thin Solid Films 515 (2006) 1470.
- [7] C. Dragoi, M. Cernea, L. Trupina, Appl. Surf. Sci. 257 (2011) 9600.
- [8] H. Huhtinen, M. Irjala, P. Paturi, M. Falter, Physica C 472 (2012) 66.
- [9] M. Yuksek, A. Elmali, M. Karabulut, G.M. Mamedov, Appl. Phys. B 98 (2010) 77.
- [10] S. Shigetomi, T. Ikari, Jpn. J. Appl. Phys. 46 (2007) 5774.
- [11] H. Ni, X.D. Li, G. Cheng, R. Klie, J. Mater. Res. 21 (2006) 2882.
- [12] H. Ni, X.D. Li, H. Gao, Appl. Phys. Lett. 88 (2006) 043108.
- [13] H. Ni, X.D. Li, J. Nano. Res. 1 (2008) 10.
- [14] S.K. Wang, T.C. Lin, S.R. Jian, J.Y. Juang, Jason.S.C. Jang, J.Y. Tseng, Appl. Surf. Sci. 258 (2011) 1261.
- [15] S.R. Jian, W.C. Ke, J.Y. Juang, Nanosci. Nanotechnol. Lett. 4 (2012) 598.
- [16] S.R. Jian, H.G. Chen, G.J. Chen, Jason.S.C. Jang, J.Y. Juang, Curr. Appl. Phys. 12 (2012) 849.
- [17] X.D. Li, B. Bhushan, Mater. Charact. 48 (2002) 11.
- [18] W.C. Oliver, G.M. Pharr, J. Mater. Res. 7 (1992) 1564.
- [19] B.D. Cullity, S.R. Stock, Element of X-ray Diffraction, Prentice Hall, New Jersey, 2001. p. 170.
- [20] D.H. Mosca, N. Mattoso, C.M. Lepienski, W. Veiga, I. Mazzaro, V.H. Etgens, M. Eddrief, J. Appl. Phys. 91 (2002) 140.
- [21] G.F. Wang, X.D. Li, Appl. Phys. Lett. 91 (2007) 231912.
- [22] X.Y. Tao, X.N. Wang, X.D. Li, Nano Lett. 7 (2007) 3172.
- [23] J. Schiotz, T. Vegge, F.D. Di Tolla, K.W. Jacobsen, Phys. Rev. B 60 (1999) 11971.
- [24] J.E. Bradby, S.O. Kucheyev, J.S. Williams, C. Jagadish, M.V. Swain, P. Munroe, M.R. Phillips, Appl. Phys. Lett. 80 (2002) 4537.
- [25] S.R. Jian, J.Y. Juang, Y.S. Lai, J. Appl. Phys. 103 (2008) 033503.
- [26] S.R. Jian, J.Y. Juang, J. Nanomater. 2012 (2012) 914184.
- [27] S.R. Jian, Nanoscale Res. Lett. 3 (2008) 6.
- [28] S.R. Jian, G.J. Chen, J.Y. Juang, Curr. Opin. Solid State Mater. Sci. 14 (2010) 69.
- [29] D. Lorenz, A. Zeckzer, U. Hilpert, P. Grau, H. Johansen, H.S. Leipner, Phys. Rev. B 67 (2003) 172101.
- [30] K.L. Johnson, Contact Mechanics, Cambridge University Press, Cambridge, UK, 1985.
- [31] G. Zhao, M. Liu, F. Yang, Acta Mater. 60 (2012) 3773.